

difference in the coordination of oxygen around Eu^{2+} ions. Also their emission intensities increase with transforming into phase IV. Particularly the quantum efficiency of $\text{SrB}_2\text{O}_4(\text{IV})\text{:Eu}^{2+}$ is about 100 times higher than that of $\text{SrB}_2\text{O}_4(\text{I})\text{:Eu}^{2+}$ under 313-nm excitation. This is due to the fact that a number of Eu^{2+} ions in $\text{SrB}_2\text{O}_4(\text{IV})\text{:Eu}^{2+}$ hardly form the clusters which contribute to the nonradiative process. The

luminescence properties of the high-pressure phases of $\text{CaB}_2\text{O}_4\text{:Eu}^{2+}$ correspond to those of the EuB_2O_4 phase pressed out into the grain boundaries of the matrix because of the crystallographic mismatch of Eu^{2+} and Ca^{2+} ions.

Registry No. EuB_2O_4 , 38313-81-4; SrB_2O_4 , 13703-84-9; CaB_2O_4 , 13701-64-9.

Contribution from the Chemical Physics Group,
Tata Institute of Fundamental Research, Bombay 400 005, India

Magnetic Susceptibility Study and Ground-State Zero-Field Splitting in Manganese(III) Porphyrins

D. V. BEHERE and SAMARESH MITRA*

Received April 17, 1979

The paper reports results of magnetic measurements on the polycrystalline (4–100 K) and single-crystal (80–300 K) samples of two typical high-spin manganese(III) porphyrins, namely, chloro(tetraphenylporphyrinato)manganese(III) and chloro(tetraphenylporphyrinato)(pyridine)manganese(III). The experimental data are analyzed in terms of spin-Hamiltonian formalism, which gives an accurate estimate of the zero-field splitting of the ground state of the manganese(III) ion as $D = -2.3$ and -3.0 cm^{-1} , respectively, in the above two compounds. The measurement of single crystal has been found to be particularly informative about the sign and magnitude of D in manganese(III) porphyrins.

Introduction

The magnetic and electronic properties of manganese porphyrins are interesting because of direct and indirect involvement of these molecules in various biological processes.¹⁻⁴ A variety of physical studies have been made on manganese(III) porphyrins with a view to understand their electronic structure and other properties. Surprisingly very little attention has been paid to their magnetic susceptibility studies⁵ even though it is recognized⁶⁻¹⁰ that such study especially on single crystals would be very valuable for understanding ground-state properties of any paramagnetic ion. A survey of existing literature shows that magnetic susceptibility studies on most manganese porphyrins are confined to measurements at room temperature (perhaps just to determine the spin state of the manganese ion); only in a few cases do the measurements extend down to 77 K. There is hardly any report of average magnetic susceptibility study on manganese porphyrins down to liquid-helium temperatures. To our knowledge no single-crystal magnetic susceptibility study on any manganese porphyrin has yet been reported even at room temperature.

In the present paper we report the results of our magnetic susceptibility measurements on polycrystalline (300–4 K) and single-crystal (300–80 K) samples of two benzene-solvated manganese(III) porphyrins, namely, chloro(5,10,15,20-tetraphenylporphyrinato)manganese(III), ClMnTPP , and chloro(5,10,15,20-tetraphenylporphyrinato)(pyridine)manganese(III), Cl(py)MnTPP . Molecular structure of the former is the usual square-pyramidal type with manganese atom being surrounded

by the four basal pyrrole nitrogens and an axial chloride ion.¹¹ In Cl(py)MnTPP hexacoordinated geometry is completed by the pyridine through a long axial Mn-N_{py} bond.¹² The experimental magnetic data on these two related systems are used to deduce zero-field splitting (ZFS) of the ground state. Conventional techniques such as ESR and Mössbauer have not been of any help in determining ZFS in the manganese(III) porphyrins. However values of this important ground-state parameter are known, for comparison, in a few manganese(III) porphyrins by far-infrared spectroscopy.¹³

Experimental Section

ClMnTPP and Cl(py)MnTPP were prepared by literature methods,¹⁴ and their identity was established by elemental analysis¹⁵ and spectra.¹⁶

Single crystals of ClMnTPP were grown from benzene solution, which readily gave large well-developed tabular single crystals weighing up to 20 mg. These crystals were found to be benzene solvate.¹⁷ Preliminary X-ray studies indicate that the crystals belong to the tetragonal system with $a = 12.9 \text{ \AA}$ and $c = 10.2 \text{ \AA}$. Cl(py)MnTPP crystals were grown from a benzene-pyridine solution,¹² which gave large (~12 mg) elongated prismatic crystals. These crystals were also benzene solvate and were established by X-rays to be of the monoclinic system with unit cell data identical with those reported.¹²

Average magnetic susceptibility of the polycrystalline samples was measured between 300 and 4 K by an automatic Oxford Faraday Instrument described in detail elsewhere.¹⁸ The magnetic anisotropy was measured between 300 and 80 K by using the null-deflection

- (1) Boucher, L. J. *Coord. Chem. Rev.* **1972**, *7*, 289.
- (2) Wang, J. H. *Acc. Chem. Res.* **1970**, *3*, 90.
- (3) Olson, J. M. *Science* **1970**, *168*, 438.
- (4) Loach, P. A.; Calvin, M. *Biochemistry* **1963**, *2*, 361.
- (5) See ref 1 for a listing of the magnetic susceptibility data.
- (6) Mitra, S. *Prog. Inorg. Chem.* **1977**, *22*, 309.
- (7) Barraclough, C. G.; Martin, R. L.; Mitra, S.; Sherwood, R. C. *J. Chem. Phys.* **1970**, *55*, 1638, 1643.
- (8) Venoyama, H.; Lizyka, T.; Morimoto, H.; Kotani, M. *Biochim. Biophys. Acta* **1968**, *160*, 159.
- (9) Behere, D. V.; Marathe, V. R.; Mitra, S. *J. Am. Chem. Soc.* **1977**, *99*, 4149.
- (10) Ganguli, P.; Marathe, V. R.; Mitra, S. *Inorg. Chem.* **1975**, *14*, 970.

- (11) Tulinsky, A.; Chen, B. M. L. *J. Am. Chem. Soc.* **1977**, *99*, 3647.
- (12) Kirner, J. F.; Scheidt, W. R. *Inorg. Chem.* **1975**, *14*, 2081.
- (13) Brackett, G. C.; Richards, P. L.; Caughey, W. S. *J. Chem. Phys.* **1971**, *54*, 4383.
- (14) Adlar, A.; Longo, F. R.; Kampas, F.; Kim, J. *J. Inorg. Nucl. Chem.* **1970**, *32*, 2443.
- (15) Microanalysis: Calcd for $\text{TPPMnCl}\cdot 2\text{C}_6\text{H}_6$: C, 78.3; H, 4.69; N, 6.52. Found: C, 77.5; H, 4.28; N, 6.2. Calcd for $\text{TPPMnCl(py)}\cdot\text{C}_6\text{H}_6$: C, 76.8; H, 4.57; N, 8.14. Found: C, 76.5; H, 4.6; N, 8.0.
- (16) Boucher, L. J. *J. Am. Chem. Soc.* **1970**, *92*, 2725.
- (17) Presence of two benzene molecules in the lattice was also confirmed by thermogravimetric analysis.
- (18) Mackey, D. J.; Evans, S.; Martin, R. L. *J. Chem. Soc., Dalton Trans.* **1976**, 1515.

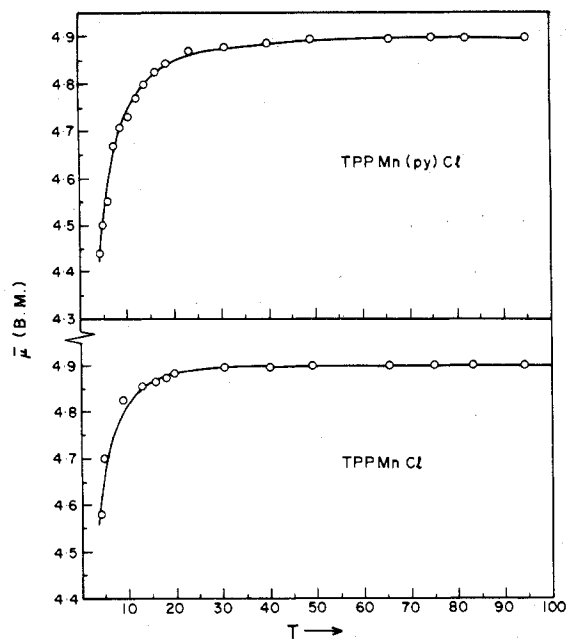


Figure 1. Temperature dependence of the average magnetic moment ($\bar{\mu}$) of ClMnTPP and Cl(py)MnTPP. The circles are the experimental data, and the solid curve is the theoretical fit (see the text).

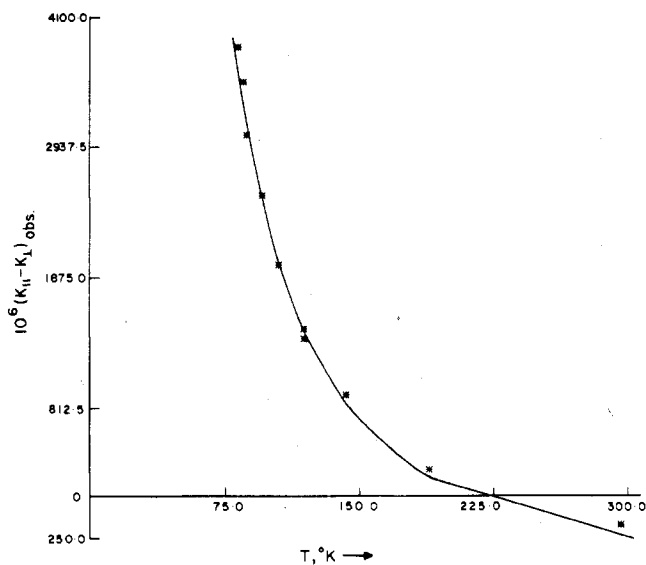


Figure 2. Temperature dependence of the observed molecule anisotropy for Cl(py)MnTPP uncorrected for the diamagnetic anisotropy of the porphyrin molecule. The solid curve is the theoretical fit (see the text).

method¹⁹ and by equipment described earlier.^{9,10} Magnetic anisotropy measurement on the tetragonal crystals of ClMnTPP showed no anisotropy in the symmetry plane, which is consistent with its crystallographic requirement. The measured anisotropy was thus taken the same as the molecular anisotropy.^{9,20} For the monoclinic crystals of Cl(py)MnTPP the anisotropy was measured in the (010) plane ($\Delta\chi_b$) with "b" axis vertical. The molecular anisotropy is then simply given by the relation¹⁹ $K_{||} - K_{\perp} = \Delta\chi_b / \sin^2 \delta$, where δ is the angle which the symmetry axis of the molecule (i.e., $K_{||}$ - axis) makes with the b axis of the crystal. Here $K_{||}$ and K_{\perp} are the molecular susceptibilities parallel and perpendicular to the symmetry axis of the molecule, respectively. For Cl(py)MnTPP, δ is calculated from the structural data¹² to be 53.7°.

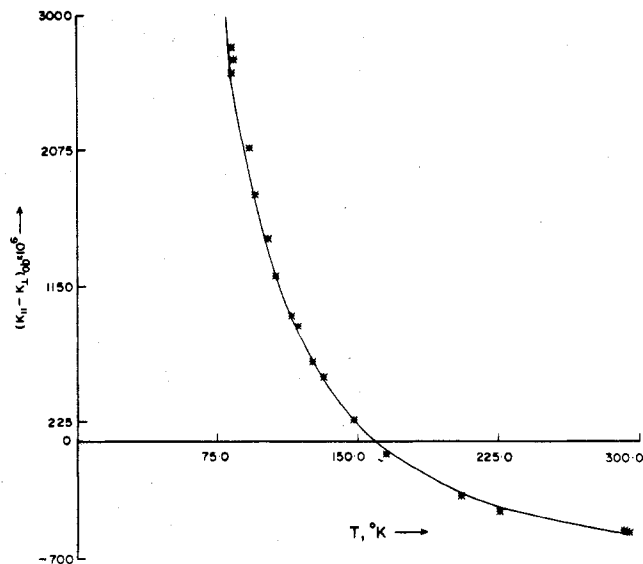


Figure 3. Temperature dependence of the observed molecular anisotropy for ClMnTPP, uncorrected for the diamagnetic anisotropy of the porphyrin molecule. The solid curve is the theoretical fit.

Results and Discussion

The results of the average magnetic susceptibility and anisotropy measurements on the two compounds are summarized in Figures 1–3.

The average magnetic moment ($\bar{\mu}$) of both the compounds at room temperature is close to the spin-only value for $S = 2$. The magnetic moment remains nearly constant down to about 15 K, below which it decreases fast. This behavior is indicative of a sizeable zero-field splitting of the ground state.

The behavior of the observed magnetic anisotropy in Figures 2 and 3 for the two compounds is similar and bears the characteristic feature that it passes through 0 in the temperature range of the study. The observed anisotropy consists of mainly two contributions, namely, the paramagnetic anisotropy due to the Mn(III) ion and the diamagnetic anisotropy of the porphyrin ring, the shape anisotropy being negligible in such systems.²¹ The diamagnetic anisotropy contribution is expected to be large in manganese(III) porphyrin, dominating the paramagnetic part at higher temperature. It is easy to see from the data in Figures 2 and 3 that the sign of paramagnetic anisotropy and diamagnetic anisotropy must be opposite. Since the sign of the diamagnetic anisotropy ($K_{\perp} - K_{||}$)_d in a π system such as porphyrin is always positive,^{22,23} it follows that the sign of the paramagnetic anisotropy in ClMnTPP and Cl(py)MnTPP must be $K_{||}^p > K_{\perp}^p$.

For the high-spin d^4 Mn(III) ion in manganese(III) porphyrin, the most likely electron configuration is $d_{xy}^1 d_{xz,yz}^2 d_{z^2}^1$ with the antibonding $d_{x^2-y^2}$ orbital lying much higher in energy. The ground state is then a spin-quintet orbital singlet. The magnetic moment at room temperature and its near constancy at higher temperatures (>20 K) in Figure 1 indicate that there is no close-lying excited state. One can then use spin-Hamiltonian formalism of the form

$$\mathcal{H} = DS_z^2 + g\beta H \cdot S \quad (1)$$

to deduce the ground-state properties of the Mn(III) ion. Here

(19) For details see, for example: Mitra, S. *Transition Met. Chem.* **1972**, 7, 183.
 (20) Lonsdale, K.; Krishnan, K. S. *Proc. R. Soc. London, Ser. A* **1936**, 156, 597.

(21) Majumdar, M. *Indian J. Phys.* **1962**, 36, 111.
 (22) Barraclough, C. G.; Martin, R. L.; Mitra, S. *J. Chem. Phys.* **1971**, 55, 1427.
 (23) Kirshnan, K. S.; Guha, B. C.; Banerjee, S. *Philos. Trans. R. Soc. London, Ser. A* **1933**, 231, 235.
 (24) Boyd, P. D. W.; Buckingham, D. A.; McMeeking, R. F.; Mitra, S. *Inorg. Chem.* **1979**, 18, 3585.

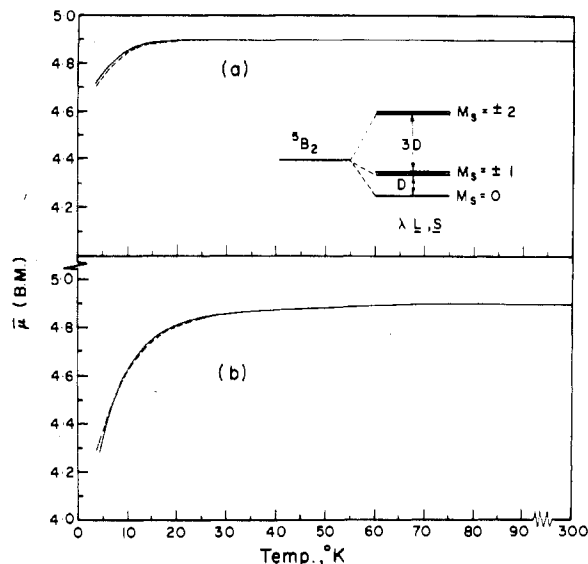


Figure 4. Temperature dependence of the average magnetic moment calculated for two typical values of D from eq 2: (a) $D = \pm 2 \text{ cm}^{-1}$; (b) $D = \pm 6 \text{ cm}^{-1}$. The full curves are for positive values of D and the broken ones for negative values of D .

D is the ZFS parameter. Due to the axial distortion and spin-orbit coupling, the $S = 2$ state is split into three zero-field split levels, $M_s = 0, \pm 1$, and ± 2 , the separation between $M_s = 0$ and ± 1 and that between $M_s = 0$ and ± 2 being D and $4D$, respectively (see the inset in Figure 4). By use of eq 1, the following equations for the principal magnetic moments ($\mu_i^2 = 7.997K_i^p T$) can be derived:

$$\mu_{\parallel}^2 = \frac{6g_{\parallel}^2(e^{-D/kT} + 4e^{-4D/kT})}{(1 + 2e^{-D/kT} + 2e^{-4D/kT})}$$

$$\mu_{\perp}^2 = \frac{g_{\perp}^2 kT}{D} \left\{ \frac{18 - 14e^{-D/kT} - 4e^{-4D/kT}}{(1 + 2e^{-D/kT} + 2e^{-4D/kT})} \right\} \quad (2)$$

Before fitting of the data, some consequences of eq 2 are worth examining. In Figure 4 temperature dependence of $\bar{\mu}$ is shown for two sets of values of D . It is observed that while the temperature dependence of $\bar{\mu}$ is sensitive particularly below 15 K to the magnitude of D , it is rather insensitive to the sign of D . Hence the average magnetic moment data alone even down to liquid-helium temperature cannot be used to determine D in manganese(III) porphyrins though such data have been found to be useful for this purpose in high-spin iron(III) porphyrins.²⁵ In Figure 5 variation of the principal magnetic moments (μ_i) with D is shown for three representative temperatures. The sign of D is clearly known once the sign of the paramagnetic anisotropy even at room temperature is determined. Further the variation in $\mu_{\parallel}^2 - \mu_{\perp}^2$ in 300–80 K is found to be adequate to allow an accurate determination of the magnitude of even small values of D . Thus the present set of magnetic anisotropy data in the 300–80 K temperature range is capable of determining both the sign and the magnitude of D since there is negligible contribution to the anisotropy from the g values; i.e., $g_{\parallel} = g_{\perp} = 2$.¹³

As deduced above, the sign of the paramagnetic anisotropy in both the compounds is $K_{\parallel}^p > K_{\perp}^p$. Hence the sign of D is negative in ClMnTPP and Cl(py)MnTPP (cf. Figure 5). The sign of the observed anisotropy near room temperature is evidently decided by the sign of the diamagnetic anisotropy and hence $K_{\perp}^{\text{obsd}} > K_{\parallel}^{\text{obsd}}$. In order to fit the experimental data of Figures 2 and 3 to eq 2, we must consider the dia-

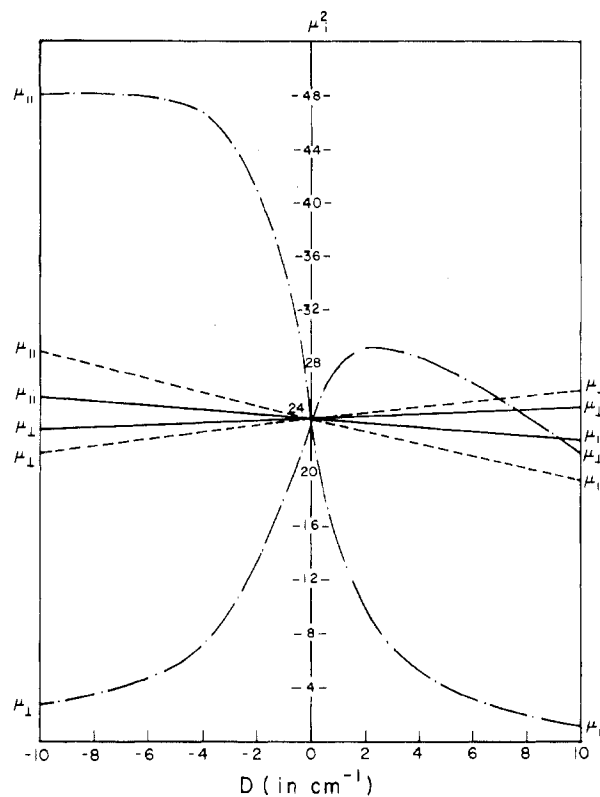


Figure 5. Variation of the principal magnetic moments with D at three typical temperatures (calculated from eq 2): —, 300 K; ---, 100 K; - - -, 10 K.

magnetic anisotropy of the molecules. The usual method of allowing for the diamagnetic anisotropy in a paramagnetic crystal is to use the anisotropy of an isostructural (or at least analogous) diamagnetic compound. We have used in the past the diamagnetic anisotropy of NiTPP for this purpose in our studies on ClFeTPP⁹ and FeTPP.²⁴ In the present case the presence of the additional benzene (solvate) and pyridine molecules (which are also expected to be anisotropic) complicates the matter. We have therefore used diamagnetic anisotropy correction as a parameter and fitted the observed anisotropy (cf. Figures 2 and 3) to eq 2. Taking $g_{\parallel} = g_{\perp} = 2$,¹³ the following values of D and $(K_{\perp} - K_{\parallel})_d$ were obtained:

	D, cm^{-1}	$10^6(K_{\perp} - K_{\parallel})_d$
ClMnTPP	-2.3 ± 0.2	620
Cl(py)MnTPP	-3.0 ± 0.3	600

The $\bar{\mu}$ data were also independently fitted by taking D to be negative (as from above results), and very similar values for D were obtained. For ClMnTPP, $D = -2.55 \text{ cm}^{-1}$, and for Cl(py)MnTPP, $D = -3.5 \text{ cm}^{-1}$ (Figure 1). The above diamagnetic anisotropies for the two manganese porphyrins appear to be quite reasonable when we compare them with the diamagnetic anisotropies of NiTPP, pyridine, and benzene (NiTPP, $\Delta K = 525$; C_6H_6 , $\Delta K = 60$; $\text{C}_5\text{H}_5\text{N}$, $\Delta K \approx 45 \times 10^{-6}$).^{19,25} An exact additive agreement is however not expected since it will depend upon the relative orientation of the benzene and pyridine molecules in the unit cell.

The sign of D in two compounds obtained from anisotropy studies is the same. Their magnitudes are also similar, and the value for ClMnTPP compares very favorably with that observed directly by infrared spectroscopy for analogous (deuteroporphyrin IX dimethyl ester)manganese(III) chloride¹³ ($D = -2.53 \text{ cm}^{-1}$). The value of D for Cl(py)MnTPP is slightly larger than that for the ClMnTPP, the difference being apparently just outside the estimated error. The difference may be a consequence of the weaker axial interaction in the Cl-

(py)MnTPP (Mn-Cl = 2.467 Å; Mn-N_{py} = 2.44 Å) as compared to the ClMnTPP (Mn-Cl = 2.363 Å). Further in Cl(py)MnTPP the manganese is displaced by only 0.12 Å from the center of the mean porphyrin plane as against 0.27 Å in the ClMnTPP, implying a stronger equatorial interaction in the former. Both these factors are expected to produce larger ZFS in the pyridine adduct as compared to the ClMnTPP.

Conclusion

The measurement of magnetic anisotropy in the liquid-nitrogen temperature range has been found to be useful in deducing accurately the sign and magnitude of the zero-field splitting parameter in manganese(III) porphyrins. If this measurement is done down to liquid-helium temperatures, a more accurate and reliable value could be deduced. On the other hand the temperature dependence of $\bar{\mu}$ even down to 4

K is unable to decide uniquely the sign of D . There appears to be not much variation in D either with the change in axial ligand or with the substitution on the porphyrin ring in ClMnTPP, Cl(py)MnTPP, and ClMnDPME. It is however interesting that the ZFS in the isoelectronic high-spin deoxyhemoglobin is rather higher and opposite in sign ($D \approx 5 \text{ cm}^{-1}$), indicating the difference in the nature of the bonding in the two cases.

Acknowledgment. The average magnetic susceptibility below 77 K was measured at Research School of Chemistry, Australian National University, Canberra, where S.M. spent a study leave during 1977-1978. We are very grateful to Professor R. L. Martin for providing the experimental facility. We also wish to thank Dr. S. N. Bhatia for his help.

Registry No. ClMnTPP, 32195-55-4; Cl(py)MnTPP, 55669-25-5.

Contribution from the Kitami Institute of Technology,
Kitami 090, Japan

Proton Nuclear Magnetic Resonance Study of Ion Hydration in Acetone. 2

K. MIURA and H. FUKUI*

Received March 9, 1979

Ab initio calculation of the shielding change of the water proton due to a point charge has been performed and compared with the experimental shifts of the ion-water associations in acetone reported in our previous paper. From the theoretical and experimental shielding changes, it was concluded that (a) anion-water associations do not occur in acetone solvent and (b) the theoretical calculation leads to a shielding change of -1.6 to -3.9 ppm, which is in qualitative agreement with the experimental results.

Introduction

Water proton nuclear magnetic resonance (¹H NMR) chemical shifts produced by diamagnetic salts in aqueous solution have been used to study the effects of electrolytes on the structure of water and the nature of water-solvent interaction.¹ According to Shoolery and Alder,² the chemical shift produced by ions in aqueous solution is the sum of at least two factors: (i) polarization of water molecules and (ii) structure breaking of the water hydrogen-bonded network, by ions. If we want to investigate the mechanism of the shielding change due to the hydration of ions, it is desirable to separate the above two contributions. In paper 1³ of this series, we showed that the structure-breaking effect is negligible in the solution of low water content in acetone solvent.

A water molecule in acetone seems to form the hydrogen bond of water hydrogen to acetone oxygen. This hydrogen bonding will obstruct water-water and water-anion associations. Therefore, we can observe the shielding change owing to water-cation bonding only. Moreover, it is possible to observe a favorable 1:1 water-cation complex formation at low water concentrations in acetone solvent. The 1:1 complex formation allows us to analyze the chemical shift changes as a function of added ion concentration and obtain the polarization shift and equilibrium constant. However, the detailed relationship between proton magnetic shielding and the geometrical configuration of the hydrated ion system is not completely understood. This places some uncertainty on conclusions resulting from the use of proton NMR spectroscopy for probing ion-water interactions. Our purpose in this study is

to perform an ab initio calculation of the shielding change of the water proton due to a point charge and compare it with the experimental results in paper 1.

In the Calculations, a brief explanation of the method used and its results are given. In the Discussion, a brief survey of experimental results in paper 1 is stated and compared with the ab initio estimates.

Calculations

A. Theory. According to the Ramsey theory of chemical shielding,⁴ the components of the shielding tensor are given by eq 1 where $\sigma_{\alpha\beta}^d$ are components of the diamagnetic term

$$\sigma_{\alpha\beta} = \sigma_{\alpha\beta}^d + \sigma_{\alpha\beta}^p \quad (1)$$

given by eq 2, where \vec{r}_O denotes the vector between the gauge

$$\sigma_{\alpha\beta}^d = 26.626 \times 10^{-6} \sum_{\mu\nu} P_{\mu\nu} \langle \mu | (\vec{r}_O \cdot \vec{r}_N \delta_{\alpha\beta} - r_{O\alpha} r_{N\beta}) r_N^{-3} | \nu \rangle \quad (2)$$

origin and electron and \vec{r}_N is the vector between nucleus N and electron. r_O and r_N are expressed here in atomic units. Components of the paramagnetic shielding tensor, $\sigma_{\alpha\beta}^p$, are given by eq 3, in atomic units, where $\vec{l}_O = \vec{r}_O \times \vec{\nabla}$ and $\vec{l}_N =$

$$\sigma_{\alpha\beta}^p = 53.251 \times 10^{-6} \sum_{\substack{i, \text{occ} \\ j, \text{unocc}}} (\epsilon_j - \epsilon_i - J_{ij} + 2K_{ij})^{-1} \times \\ \sum_{\mu\nu\lambda\sigma} C_{\mu}^* C_{\nu} C_{\lambda}^* C_{\sigma} \langle \mu | r_N^{-3} l_{N\alpha} | \nu \rangle \langle \lambda | l_{O\beta} | \sigma \rangle + \\ \langle \mu | l_{O\alpha} | \nu \rangle \langle \lambda | r_N^{-3} l_{N\beta} | \sigma \rangle \quad (3)$$

$\vec{r}_N \times \vec{\nabla}$. Other notations conform to those in the formula by Barfield and Grant.⁵ Integrals of the following types occur in eq 2 and 3: (i) $\langle \mu | r_N^{-3} x_{O\alpha} y_{N\beta} | \nu \rangle$; (ii) $\langle \mu | x_O (\partial/\partial y_O) | \nu \rangle$; (iii)

(1) J. F. Hinton and E. S. Amis, *Chem. Rev.*, **67**, 367 (1967).

(2) J. N. Shoolery and B. J. Alder, *J. Chem. Phys.*, **23**, 805 (1955).

(3) H. Fukui, K. Miura, T. Ugai, and M. Abe, *J. Phys. Chem.*, **81**, 1205 (1977).

(4) N. F. Ramsey, *Phys. Rev.*, **78**, 699 (1950).

(5) M. Barfield and D. M. Grant, *J. Chem. Phys.*, **67**, 3322 (1977).